

# Elaboration of Amorphous-Clay Hybrid: ( $\text{Al}_2\text{Si}_2\text{O}_7 \cdot 1/2\text{Li}_2\text{O}$ ) Designed as a Single Ion Conducting Solid Electrolyte for Li-Ion Batteries

Nouha Jaafar, Sonia Naamen, Hafsia Ben Rhaïem, Abdesslem Ben Haj Amara\*

Laboratory of Physics of Lamellar Hybrid Materials and Nanomaterials, Department of Physics, Faculty of Science of Bizerte, University of Carthage, Bizerte, Tunisia  
Email: [\\*abdesslem.bamara@fsb.rnu.tn](mailto:abdesslem.bamara@fsb.rnu.tn)

Received 29 September 2014; revised 15 November 2014; accepted 30 November 2014

Copyright © 2014 by authors and Scientific Research Publishing Inc.  
This work is licensed under the Creative Commons Attribution International License (CC BY).  
<http://creativecommons.org/licenses/by/4.0/>



Open Access

---

## Abstract

Keying of lithium chloride alkali halide salt into the interlamellar space of nacrite clay mineral leads to a stable hybrid material that after calcination under inert atmosphere at 723 - 873 K induces an amorphous metahybrid. The electrochemical impedance spectroscopy (EIS) was performed to investigate the electric/dielectric properties of the hybrid with various parameters: frequency and temperature. Equivalent circuit was proposed to fit the EIS data. The experiment results show that the ionic conduction mechanism is related to the motion of  $\text{Li}^+$  cations which are thermally activated, named *the hopping model*. Furthermore, the resulting metahybrid obtained from dehydroxylation of the formal hybrid shows a superionic behavior with high ionic conductivity up to  $10^{-2} \text{ S} \cdot \text{m}^{-1}$ , good electrochemical stability and can be used as a solid electrolyte material for Li-ion batteries.

## Keywords

Nacrite, Clay, Hybrid, Amorphous, Solid Electrolyte, Lithium-Ion Battery

---

## 1. Introduction

Over the past three decades, much attention has been paid to solid electrolytes instead of liquid electrolytes be-

---

\*Corresponding author.

cause of their potential use in the electrochemical power sources (batteries, lithium ion cells, lithium batteries, fuel cells, electrochemical sensors, etc.) [1]. Their advantages include longer life, high energy density and no possibility of leak, etc. They are suitable in compact power batteries used in pace-makers, mobile telephones and laptops [2].

In order to improve the bulk properties of solid electrolytes, a good number of researchers are interested in the synthesis and characterization of lithium-ion conductors based on different classes of materials such as ceramics, polymers, glasses and so on [1]. They are motivated by the small ionic radius of  $\text{Li}^+$  cation, its low weight, ease of motion and its appliance in high energy density batteries [3]-[8].

However, there are rare studies concerning solid state electrolytes based on clay materials [4]-[8], such as: poly(vinylidene fluoride-hexafluoropropylene)/organo-montmorillonite nanocomposite as a polymer electrolyte [4], poly(ethylene oxide)/intercalated clay as a polymer electrolyte [5], organophilic vermiculite/poly(methyl-methacrylate)/1-butyl-3-methylimidazolium hexafluorophosphate composite as a gel polymer electrolyte [6], poly(vinylidene fluoride) based nanocomposite porous polymer as a polymer electrolyte in lithium ion batteries [7] and poly(vinylidene fluoride)-clay nanocomposite as a gel polymer electrolyte for Li-ion batteries [8], etc. Otherwise, applications of kaolin-type clay in electronic devices have not been reported. Therefore, we are proposing to innovate a new class of conductors based on nacrite-polytype clay.

Nacrite is a 1:1 dioctahedral aluminosilicate that belongs to the kaolin group, which also includes dickite and kaolinite [9]. Kaolin [ $\text{Si}_2\text{Al}_2\text{O}_5(\text{OH})_4$ ] is a 1:1 layered phyllosilicate and is the most abundant and ubiquitous clay mineral in soils and sediments. One side of the layer is gibbsite-like with aluminium atoms octahedrally coordinated to corner oxygen atoms and hydroxyl groups. The other side of the layer constitutes a silica-like structure in which the silicon atoms are tetrahedrally coordinated to oxygen atoms. The adjacent layers are linked via hydrogen bonds ( $\text{O}-\text{H}\cdots\text{O}$ ) involving aluminol ( $\text{Al}-\text{OH}$ ) and siloxane ( $\text{Si}-\text{O}$ ) groups. As a consequence of this structure, the silica/oxygen and alumina/hydroxyl sheets are exposed and interact with different components in the soil [10].

The intercalation of clay with salts of alkali halides and its correlation with ionic conduction has shown to be important phenomena to design novel hybrid materials combining good electrochemical window with stable structural properties [11]. Nacrite is subsequently selected among the kaolin host minerals for its high chemical stability and its well-packed structure which is considered suitable for the incorporation of guest species [12]-[14].

This current paper is a sequel of our previous paper [15] concerning the synthesis and the structural characterization of the elaborated nacrite-LiCl hybrid by means of X-ray diffraction simulation, TG analysis and infrared spectroscopy.

The purpose of this paper is to study the electrochemical properties of the functionalized nacrite-LiCl hybrid. In this regard, we carry out the electric impedance ( $Z'$ ,  $Z''$ ), the electrical conductivity ( $\sigma_{ac}$ ,  $\sigma_{dc}$ ) and the dielectric permittivity ( $\epsilon'$ ,  $\epsilon''$ ) measurements of the elaborated hybrid. Therefore, understanding the mechanism of conduction is crucial.

## 2. Experimental

### 2.1. Materials

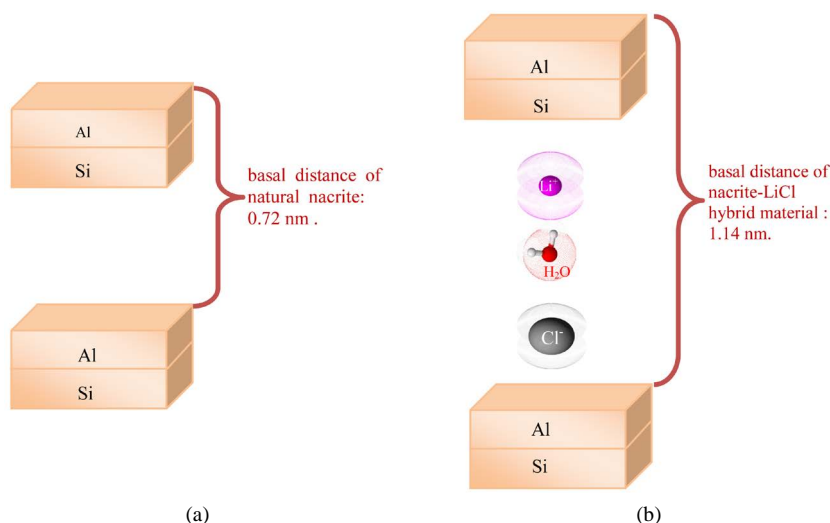
#### 2.1.1. Nacrite: Starting Tunisian Clay Material

Well-crystallized Tunisian nacrite [ $\text{Si}_2\text{Al}_2\text{O}_5(\text{OH})_4$ ] is used in this research (Scheme 1(a)). This layered clay mineral has been previously described and characterized [16]-[20].

#### 2.1.2. Nacrite-LiCl Hybrid: Starting Hybrid

The experimental protocol followed to synthesize the stable nacrite-LiCl hybrid material have been elucidated in our recent work [15], where the nacrite intercalation process detailed by *Ben Haj Amara* has been carefully adopted [16]. The **nacrite-LiCl hybrid** (Scheme 1(b)) obtained at room temperature has been corroborated by X-ray diffraction: the actual composition was found to be [ $\text{Si}_2\text{Al}_2\text{O}_5(\text{OH})_4 \cdot (1-\alpha)\text{LiCl} \cdot (1-\alpha)\text{H}_2\text{O}$ ], ( $\alpha = 0.14$ ) with a basal distance equals to 1.14 nm [15].

Noting that the *in-situ* heat-treatment of the nacrite-LiCl hybrid at the temperature of 523 K is accompanied with the removal of the intercalated water molecules [15]. The structural composition becomes [ $\text{Si}_2\text{Al}_2\text{O}_5(\text{OH})_4 \cdot (1-\alpha)\text{LiCl}$ ], where ( $\alpha = 0.14$ ).



**Scheme 1.** (a) Schematic representation of the gibbsite and silica-like layers of the nacrite sample; (b) Schematic representation of the nacrite-LiCl hybrid.

### 2.1.3. Amorphous Nacrite-LiCl Hybrid

Knowing that the calcination of Tunisian **nacrite** around the temperature of 823 K leads to amorphous synthetic phase, commonly named **metanacrite** characterized with a disordered polymerized silicon/aluminum framework [20]. In the same line, the calcination of the **nacrite-LiCl hybrid** around this temperature from 723 - 873 K leads to amorphous synthetic phase of the clay hybrid [15]:

1) Metanacrite-LiCl hybrid:

The *in-situ* heat-treatment of the nacrite-LiCl hybrid at the transition-temperature of 723 K leads to the removal of structural water from the sample. The nacrite-LiCl hybrid is then converted to **metanacrite-LiCl hybrid** (Scheme 2) with a structural formula, deduced from TGA [15],  $[\text{Si}_2\text{Al}_2\text{O}_7 \cdot (1-\alpha)\text{LiCl}]$ , ( $\alpha = 0.14$ ).

2) Metanacrite-Li<sub>2</sub>O hybrid:

Proceeding with the *in-situ* heat-treatment of the nacrite-LiCl hybrid from 723 to 873 K generates the complete dehydroxylation and the evaporation of chlorine anions as determined with the TG analysis [15]. This phenomenon leads to the increase of amorphicity and the production of **metanacrite-Li<sub>2</sub>O hybrid** (Scheme 2)

with a structural formula  $\text{Si}_2\text{Al}_2\text{O}_7 \cdot \frac{1}{2}\text{Li}_2\text{O}$ .

## 2.2. Characterization Methods

To get maximum information about the electrical properties of the new nacrite-LiCl hybrid, the electrical impedance and the dielectric permittivity provide a wide scope of graphical analysis concerning these properties.

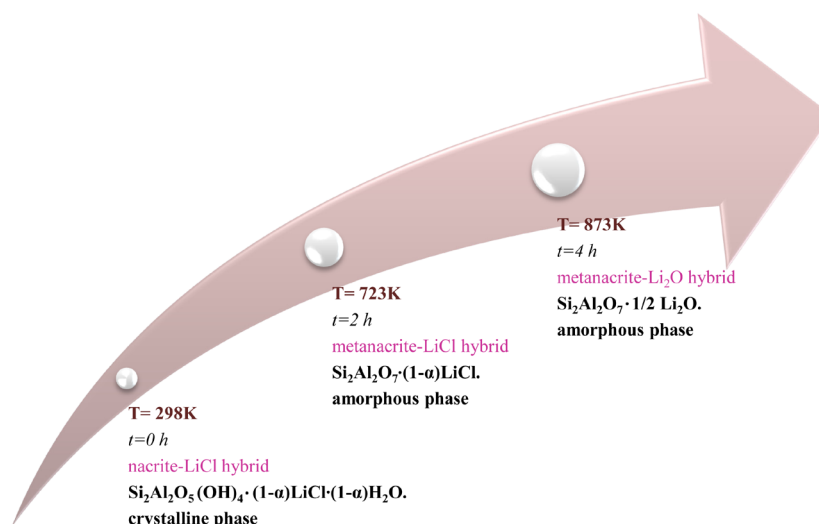
Electrochemical Impedance Spectra (EIS) were obtained using a Hewlett-Packard (HP) 4192 analyzer. The impedance measurements were taken in an open circuit using two electrode configurations with signal amplitude of 50 mV and a frequency band ranging from 10 Hz to 13 MHz at different temperatures. The examined sample is pressed into pellet using a hydraulic press. To ensure good electrical contact between the sample and the electrical junctions, the pellet was sandwiched between two platinum electrodes to form a symmetrical cell. The cell was placed into a programmable oven coupled with a temperature controller from ambient to 873 K. The resulting data were fitted using the equivalent circuit of the *Z view* software.

The analytical background used in the electrical data analysis was the following:

- The total conductivity  $\sigma_t$  can be expressed using Jonscher's law [21] [22] as:

$$\sigma_t = \sigma_{dc} + A\omega^s = \sigma_{dc} + \sigma_{ac} \quad (1)$$

where,  $\sigma_{ac}$  is the *ac* conductivity due to the hopping conduction,  $\sigma_{dc}$  is the conductivity due to the direct current,  $A$  is the temperature dependent parameter which determines the strength of polarization, while the exponent  $s$  represents the degree of interaction between mobile ions with the sample matrix.



**Scheme 2.** Schematic representation of the thermal transformations of heat-treated nacre-LiCl hybrid from room temperature to 873 K.

- The *ac* conductivity was calculated using the empirical relation [23]:

$$\sigma_{ac} = \frac{g}{R} = \frac{\left(\frac{d}{S}\right)}{R} = \frac{d}{\pi r^2 R} \quad (2)$$

where *g* is the geometric factor, *d* corresponds to the thickness of the pellet, *r* the radius of the pellet, *S* the area of the pellet and *R* the resistance.

- The temperature dependence of the *ac* conductivity was determined using the Arrhenius expression [24]:

$$\sigma_{ac} = \sigma_0 \exp\left(\frac{-E_{a(ac)}}{k_B T}\right) \quad (3)$$

where the  $E_{a(ac)}$  can be calculated from the slope of  $\log(\sigma_{ac})$  versus  $(1000/T)$ .

- The temperature dependence of the *dc* conductivity was adjusted by the Mott's equation [23] [25]:

$$\sigma_{dc} = \frac{\sigma_0}{T} \exp\left(\frac{-E_{a(dc)}}{k_B T}\right) \quad (4)$$

where  $E_{a(dc)}$  is the activation energy for *dc* conductivity,  $k_B$  is the Boltzmann's constant and *T* the temperature in Kelvin,  $\sigma_0$  is called the pre-exponential factor.

- The complex permittivity of the sample is given by the relation [23]:

$$\varepsilon^*(\omega) = \varepsilon'(\omega) - j\varepsilon''(\omega) \quad (5)$$

The dielectric permittivity characterization was interpreted according to the following expressions:

$$\varepsilon' = \frac{-Z''}{C_0(Z'^2 + Z''^2)\omega} \quad (6)$$

$$\varepsilon'' = \frac{Z'}{C_0(Z'^2 + Z''^2)\omega} \quad (7)$$

where,  $\varepsilon'(\omega)$  is the real part of dielectric permittivity and  $\varepsilon''(\omega)$  is the imaginary part of the dielectric permittivity,  $Z'$  is the real part of the electric impedance,  $Z''$  is the imaginary part of the electric impedance and  $j^2 = -1$ .  $C_0 = \varepsilon_0 S/d$  is the capacitance of the empty cell,  $\omega$  is the angular frequency,  $\varepsilon_0$  is the dielectric permittivity of free space ( $8.85418782 \times 10^{-12}$  F·m<sup>-1</sup>), *S* is the electrode surface and *d* is the distance between

the two plane electrodes.

### 3. Results and Discussion

The correlation between the electrical and dielectric properties of the nacrite-LiCl hybrid was the main purpose of this section starting with the electric impedance.

#### 3.1. Impedance Analysis

With the  $(-Z'')$  versus  $Z'$  representations (Figure 1(a) and Figure 1(b)), we observed the existence of semi-circles in the complex plane from 548 K to 873 K. At high temperature, these semi-arcs shift towards higher frequencies with a significant reduction of their size. We point out, that nacrite-LiCl hybrid becomes more conductive at high temperature. We think that this phenomenon is attributed to the existence of a deformation (destruction) of some physical characteristics of the host clay material framework and to some chemical characteristics of LiCl alkali halide.

Mathematically, the impedance diagrams for the nacrite-LiCl hybrid are studied using a fit procedure. The equivalent circuit allows the establishment of correlations between electrochemical parameters and characteristic impedance elements [26].

In the temperature range 473 - 873 K, the equivalent circuit that best adequates the response of our hybrid sample is:  $R_s // (CPE, R_p)$ .  $R_s$  represents the grain resistance connected in series and  $R_p$  the grain resistance connected in parallel to an intuitive element, called capacity of the fractal interface (CPE) (Figure 2). The (CPE)

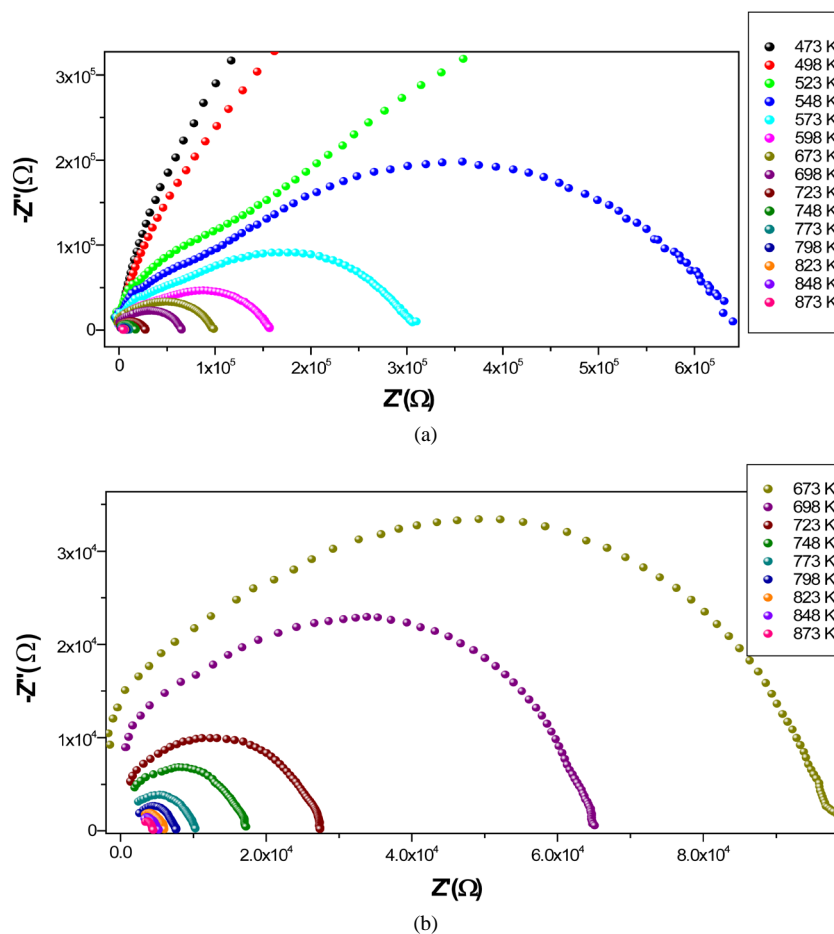


**Figure 1.** (a) Nyquist diagram of nacrite-LiCl hybrid at a temperature range from 473 to 873 K; (b) Enlargement of the Nyquist diagram of nacrite-LiCl hybrid at a temperature range from 673 to 873 K.

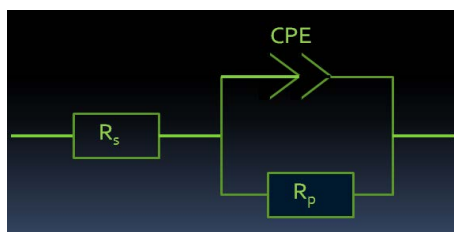


**Figure 2.** The equivalent circuit corresponding to the nacrite-LiCl hybrid from 473 to 873 K.

element accounts for the observed depression of semicircles and also the non-ideal electrode geometry. The impedance of this constant phase element is represented in Equation (8):

$$Z_{CPE} = \frac{1}{Y_0 (j\omega)^\beta} \quad (8)$$

where  $Y_0$  is the admittance ( $1/|Z|$ ) at  $\omega = 1$  rad/s and  $\beta$  a value between 0 and 1.

### 3.2. Electrical Conductivity

The  $\sigma_{dc}$  of nacrite-LiCl hybrid increases from  $(4.02 \times 10^{-6} \text{ S}\cdot\text{m}^{-1})$  at 523 K to the  $(0.11 \times 10^{-2} \text{ S}\cdot\text{m}^{-1})$  at 873 K (Table 1).

An Arrhenius behavior was observed for the hybrid. The  $E_{a(dc)}$  was determined from the slope of  $\log(\sigma_{dc} \cdot T)$  versus  $(1000/T)$  (Figure 3(a) and Figure 3(b)) and were found 0.84 eV and 0.82 eV, respectively below and above 673 K (Table 2). The obtained values suggest an ionic conduction process.

The *ac* conductivity measurements at high frequencies (1 MHz) show that  $\sigma_{ac}$  increases from  $1.22 \times 10^{-4} \text{ S}\cdot\text{m}^{-1}$  at 523 K to  $0.13 \times 10^{-2} \text{ S}\cdot\text{m}^{-1}$  at 873 K (Table 1). This remarkable increase is also related to the increase of the number of free ions in the hybrid matrix in terms of temperature.

The  $E_{a(ac)}$  (Table 2), calculated in agreement with Equation (3), corresponds to the free energy barrier an ion has to overcome for a successful jump from one site to another. These values designate that the ionic transport mechanism can be interpreted by the thermally activated hopping process [27].

Subsequently, these electrical measurements are classified in two domains: **1**) before 723 K, nacrite-LiCl hybrid behaves as a good ionic conductor and **2**) after 723 K, the amorphous nacrite-LiCl hybrid acts as a fast ionic conductor. According to these experimental results, we deduce that the disordered hybrid bears easier motion than the ordered one. We conclude that contribution of disorder and defects in the hybrid framework are responsible for the motion of charge carriers; this result is in agreement with the previous publication of *Kumar & Yashonath* [2].

In general, both cations and anions can be carriers of electric current in ionic solids. Applying the simple logic that “smaller ions diffuse faster” and since cations have smaller **ionic radii** than anions, the majority of superionic solids discovered are cation conductors [2]. Another factor that influences the diffusivity of ion is **the magnitude of charge** it carries. When the charge of an ion is large, it is likely to be confined to its site by stronger Coulombic attraction of its neighboring ions (which are of opposite charge) [2]. That is why the predominant current conducting species in known superionic solids are monovalent cations [2].

In the following part, we investigate the charge carriers responsible for conduction in our hybrid before and after the temperature of dehydroxylation.

- Before 723 K, **nacrite-LiCl hybrid** displays well-packed layers (Table 3) [15]. Vibrational spectra of the hybrid recorded using infrared spectroscopy provide valuable insights about the interactions between the nacrite host matrix and the intercalated species [15]:

- 1) Two layers of the same sheet are bound together by the tetrahedral oxygen atom common with the edge-shared octahedra [28].

- 2) Hydrogen bonding between the OH groups of the oxide/hydroxide ( $\text{Al}_2(\text{OH})_4$ ) octahedrons and the intercalated anions [15] [29] [30].

- 3) Electrostatic interactions between the basal siloxane oxygen of the gibbsite-like layer and the intercalated cations [15] [29] [30].

**Table 1.** The  $dc$  conductivity ( $\sigma_{dc}$ ),  $ac$  conductivity ( $\sigma_{ac}$ ) values at 1 MHz of nacrite-LiCl hybrid from 523 - 873 K.

Temperature range 523 - 873 [K]		
T [K]	$\sigma_{dc}$ ( $S \cdot m^{-1}$ )	$\sigma_{ac}$ ( $S \cdot m^{-1}$ ) (1 MHz)
523	$4.02 \times 10^{-6}$	$1.22 \times 10^{-4}$
548	$8.10 \times 10^{-6}$	$1.24 \times 10^{-4}$
573	$1.67 \times 10^{-5}$	$1.33 \times 10^{-4}$
598	$3.31 \times 10^{-5}$	$1.47 \times 10^{-4}$
673	$5.24 \times 10^{-5}$	$9.57 \times 10^{-5}$
698	$7.96 \times 10^{-5}$	$1.41 \times 10^{-4}$
723	$1.44 \times 10^{-4}$	$2.15 \times 10^{-4}$
748	$2.20 \times 10^{-4}$	$3.21 \times 10^{-4}$
773	$3.18 \times 10^{-4}$	$4.45 \times 10^{-4}$
798	$5.05 \times 10^{-4}$	$6.69 \times 10^{-4}$
823	$6.62 \times 10^{-4}$	$8.89 \times 10^{-4}$
848	$8.49 \times 10^{-4}$	$1.11 \times 10^{-3}$
873	$0.11 \times 10^{-2}$	$0.13 \times 10^{-2}$

**Table 2.** The  $ac$  and  $dc$  activation energies values from 508 to 873 K of nacrite-LiCl hybrid material.

Sample: nacrite-LiCl hybrid material.		
Temperature region [K]	$E_{a(dc)}$ (eV) ( $\pm 0.01$ eV)	$E_{a(ac)}$ (eV) ( $\pm 0.01$ eV) (at 1 MHz)
508 - 668 K	0.84	0.51
673 - 873 K	0.82	0.71

$E_{a(dc)}$ :  $dc$  activation energy.  $E_{a(ac)}$ :  $ac$  activation energy.

**Table 3.**  $ac$  conductivity values and structure type of the elaborated hybrids.

Hybrid	$\sigma_{ac}$ ( $S \cdot m^{-1}$ ) at 1 MHz	Structure type
$Si_2Al_2O_5(OH)_4 \cdot (1-\alpha)LiCl$	$1.22 \times 10^{-4}$	crystalline
$Si_2Al_2O_7 \cdot (1-\alpha)LiCl$	$2.15 \times 10^{-4}$	amorphous
$Si_2Al_2O_7 \cdot \frac{1}{2}Li_2O$	$0.13 \times 10^{-2}$	amorphous

So, owing to these strong interactions, the structural  $O^{2-}$ ,  $H^+$  and  $OH^-$  ions of the **alumino-silicate** fairly rigid framework are localized around their equilibrium sites, *i.e.*, they cannot escape from their lattice sites. Besides,  $H^+$  and  $OH^-$  ions of the intercalated water molecules are eliminated due to the dehydration starting from 373 K as demonstrated by TG analysis [15]. Furthermore,  $Li^+$  is known as an excellent current carrying ion in superionic solids motivated by its small ionic radius of 0.076 nm, lower weight and ease of motion [2] but  $Cl^-$  anion appears to be rather less mobile than the cation due to its great ionic radius equals to 0.181 nm [2]. To conclude,  $Li^+$  is the predominant current carrier in Li-hybrid conductor at low temperatures.

- In the temperature range between 723 - 873 K, calcination occurs, nacrite-LiCl hybrid converts to metanacrite-LiCl hybrid and then to metanacrite- $Li_2O$  hybrid containing large amount of amorphous **silico-aluminates**; therefore disorder and/or defects arise. TG investigations indicated that, in this range of temperature, dehydroxylation is accompanied by the removal of the inner-surface hydroxyls and the inner hydroxyls from the basic nacrite structure [15]. Therefore,  $OH^-$  and  $H^+$  ions do not contribute to the ionic conduction process. Besides, a new **Si-O-Al** bond is created during dehydroxylation, which prevents  $O^{2-}$  anions to contribute to the transport mechanism.

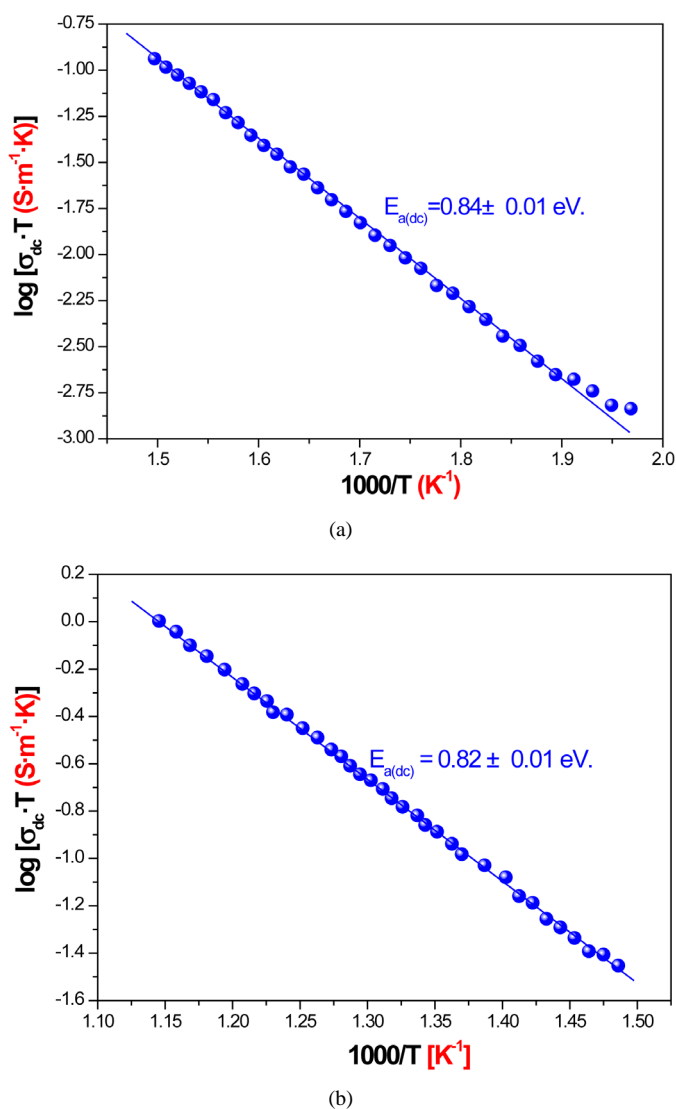


**Figure 3.** (a)  $\log(\sigma_{dc} \cdot T) = f(1000/T)$  of nacrite-LiCl hybrid material at a temperature range from 508 to 668 K. (b)  $\log(\sigma_{dc} \cdot T) = f(1000/T)$  of nacrite-LiCl hybrid material at a temperature range from 673 to 873 K.

Hence, concerning **Si<sub>2</sub>Al<sub>2</sub>O<sub>7</sub>·(1-α)LiCl hybrid** (Table 3), the associated ionic conductivity is found to increase significantly in terms of temperature, which is reasonable since the amorphous structure is so suited for easy motion of Li<sup>+</sup> ions. Besides, a clear conductivity jump is found at 723 K, which could be ascribed as the transition for the hybrid from the crystalline phase to the amorphous one.

Moreover, the **Si<sub>2</sub>Al<sub>2</sub>O<sub>7</sub> · 1/2 Li<sub>2</sub>O hybrid** showed higher conductivity (Table 3). This phenomenon can be explained by the presence of Li<sub>2</sub>O content in its framework. The presence of lithium oxide cleaves the structure and disturbs the bonding between the hybrid forming cations and oxygen anions. This alkali metal oxide increases the number of non-bridging oxygen than bridging oxygen in the amorphous hybrid matrix [31]-[33]. This enhanced conductivity might be associated with the increase in the non-bridging oxygen (NBOs) and the resulting improved Li<sup>+</sup> ion mobility [34].

Finally, Li<sup>+</sup> is the common current carrier via hopping from one site to the next for both “metanacrite-LiCl hybrid” and “metanacrite-Li<sub>2</sub>O hybrid”. Since the “metanacrite-Li<sub>2</sub>O-hybrid” phase is more amorphous than the

“metanacrite-LiCl-hybrid” phase therefore it produces greater ionic conductivity (Table 3). This shows that the conductivity was preferably affected by the amorphicity of the metanacrite framework through which mobile lithium ions may migrate.

### 3.3. Dielectric Permittivity

The study of the dielectric permittivity in ion conducting clay composite materials is very interesting to understand the ionic transport properties of materials. The real ( $\epsilon'$ ) and imaginary ( $\epsilon''$ ) part of dielectric permittivity for nacrite-LiCl hybrid material at different temperatures and frequencies are shown in (Figure 4 and Figure 5), respectively.

According to *Leluk et al.*, [28], heating of kaolin-type clay minerals from room temperature to 873 K results in a gradual decrease in the dielectric permittivity [28]. A significant volume of the structural water was removed from the aluminium silicate and gibbsite layers. The decomposition of the material produces defects that liberated a small distance movement. Consequently, the dielectric permittivity decreases considerably.

At low frequencies (Figure 4), nacrite-LiCl hybrid exhibits a decrease in the dielectric permittivity in terms of

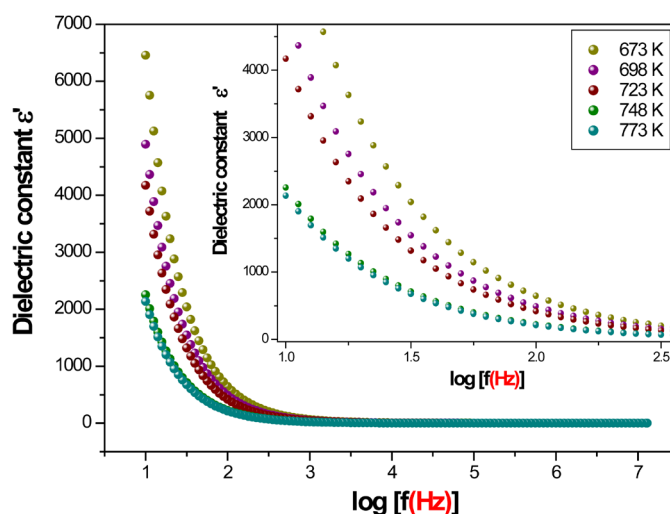


Figure 4.  $\epsilon' = f(\log f)$  of nacrite-LiCl hybrid nanomaterial at a temperature range from 673 to 773 K.

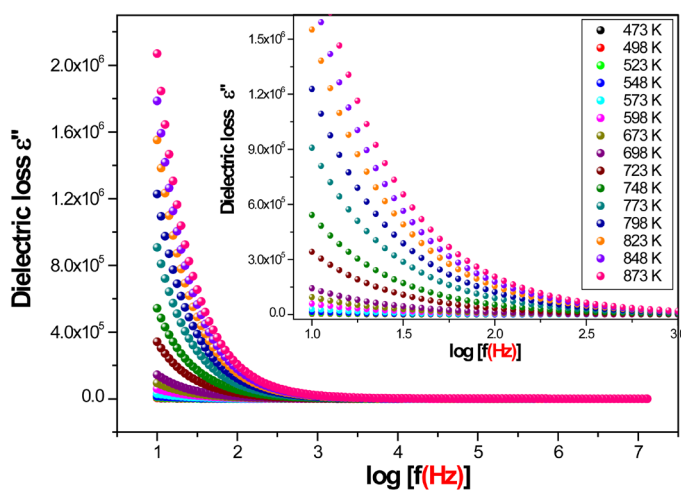


Figure 5.  $\epsilon'' = f(\log f)$  of nacrite-LiCl hybrid material at the temperature range from 473 to 873 K.

temperature related to the removal of OH groups within the temperature of dehydroxylation. On the other hand, the dielectric loss (Figure 5) increases in terms of temperature, this result corroborates the *ac* conductivity investigation of the examined sample and can be attributed to the increase in charge carrier density due to the increase of free ions in the hybrid matrix [35]. This result confirms the thermal behavior of the studied hybrid consisting in the destruction of the crystalline structure of the hybrid as a function of temperature and thus a faster movement of the lithium cations should be expected. However, **at high frequencies** (Figure 4), the dielectric constant remains invariant with temperature, whereas the dielectric loss (Figure 5) drops and becomes almost temperature independent for  $f > 10^3$  Hz. This behavior may be due to the fact that in the high frequency range, the charge carriers cannot follow the electric field.

### 3.4. Application of Metanacrite-Li<sub>2</sub>O Hybrid as a Solid Electrolyte for Lithium-Ion Battery

**Si<sub>2</sub>Al<sub>2</sub>O<sub>7</sub> · 1/2Li<sub>2</sub>O** hybrid's highly conductivity ( $\sigma_{ac} \sim 10^{-2} \text{ S} \cdot \text{m}^{-1}$ ) makes it excellent candidate as electrolyte solid for lithium-ion batteries. Furthermore, this amorphous-type Li-ion conductor offers several advantages such as: low cost and ease of handling. Its use instead of the conventional superionic conductors can drastically improve the safety aspects of lithium batteries.

## 4. Conclusions

In this work, electrical experiments are conducted in order to characterize the electrochemical properties of a new nacrite-LiCl hybrid as a function of temperature and frequency. The investigation of the *ac* and *dc* conductivity of nacrite-LiCl hybrid suggests that the suppression in the degree of crystallinity of the elaborated hybrid improves dramatically the ionic conduction which is about ten orders of magnitude larger than the low temperature conductivity value. The activation energies for conduction measured at different temperatures indicate that the conduction mechanism is driven by hopping of Li<sup>+</sup> ions from one site to the neighboring one. The dielectric constant and dielectric loss calculations support these *ac* and *dc* results.

The “metanacrite-Li<sub>2</sub>O-hybrid” with a typical composition **Si<sub>2</sub>Al<sub>2</sub>O<sub>7</sub> · 1/2Li<sub>2</sub>O** exhibits good ionic conductivity. This can be used as an innovative solid electrolyte in lithium batteries and other electrochemical devices.

## Acknowledgements

N. Jaafar acknowledges Dr. **Manuel Pedro F. Graça** (*Physics Department, University of Aveiro, Campus Universitario de Santiago 3810-193 Aveiro Portugal*) for helpful discussions and corrections.

## References

- [1] Minami, T., Tatsumisago, M., Iwakura, C., Kohjiya, S. and Tanaka, I. (2005) *Solid State Ionics for Batteries*. Springer, Berlin. <http://dx.doi.org/10.1007/4-431-27714-5>
- [2] Kumar, P.P. and Yashonath, S. (2006) Ionic Conduction in the Solid State. *Journal of Chemical Science*, **118**, 135-154. <http://dx.doi.org/10.1007/BF02708775>
- [3] Ghosh, A. and Kofinas, P. (2008) PEO Based Block Copolymer as Solid State Lithium Battery Electrolyte. *ECS Transactions*, **11**, 131-137.
- [4] Wang, M., Zhao, F., Guo, Z. and Dong, S. (2004) Poly(Vinylidene Fluoride-Hexafluoropropylene)/Organo-Montmorillonite Clays Nanocomposite Lithium Polymer Electrolytes. *Electrochimica Acta*, **49**, 3595-3602. <http://dx.doi.org/10.1016/j.electacta.2004.03.028>
- [5] Morena, M., Quijadad, R., Anaa, M.A.S., Benaventea, E., Romeroe, P.G. and González, G. (2011) Electrical and Mechanical Properties of Poly(Ethylene Oxide)/Intercalated Clay Polymer Electrolyte. *Electrochimica Acta*, **58**, 112-118. <http://dx.doi.org/10.1016/j.electacta.2011.08.096>
- [6] He, P., Chen, B., Wang, Y., Xie, Z. and Dong, F. (2013) Preparation and Characterization of a Novel Organophilic Vermiculite/Poly(Methyl Methacrylate)/1-Butyl-3-Methylimidazolium Hexafluorophosphate Composite Gel Polymer Electrolyte. *Electrochimica Acta*, **111**, 108-113. <http://dx.doi.org/10.1016/j.electacta.2013.07.192>
- [7] Prasanth, R., Shubha, N., Hng, H. H. and Srinivasan, M. (2013) Effect of Nano-Clay on Ionic Conductivity and Electrochemical Properties Of Poly(Vinylidene Fluoride) Based Nanocomposite Porous Polymer Membranes and Their Application as Polymer Electrolyte in Lithium Ion Batteries. *European Polymer Journal*, **49**, 307-318. <http://dx.doi.org/10.1016/j.eurpolymj.2012.10.033>

- [8] Deka, M. and Kumar, A. (2011) Electrical and Electrochemical Studies of Poly (Vinylidene Fluoride)-Clay Nanocomposite Gel Polymer Electrolytes for Li-Ion Batteries. *Journal of Power Sources*, **196**, 1358-1364. <http://dx.doi.org/10.1016/j.jpowsour.2010.09.035>
- [9] Elbokl, T.A. and Detellier, C. (2008) Intercalation of Cyclic Imides in Kaolinite. *Journal of Colloid and Interface Science*, **323**, 338-348. <http://dx.doi.org/10.1016/j.jcis.2008.04.003>
- [10] Wypych, F. and Satyanarayana, K.G. (2004) Clay Surfaces, Fundamentals and Applications. Academic Press/Elsevier, Waltham/Amsterdam.
- [11] Choudhary, S. and Sengwa, R.J. (2011) Ionic Conduction and Relaxation Processes in Melt Compounded Poly(Ethylene Oxide)-Lithium Perchlorate Trihydrate-Montmorillonite Nanocomposite Electrolyte. *Indian Journal of Engineering and Materials Sciences*, **18**, 147-156.
- [12] Gimenes, M.A., Profeti, L.P.R., Lassali, T.A.F., Graeff, C.F.O. and Oliveira, H.P. (2001) Synthesis Characterization, Electrochemical and Spectroelectrochemical Studies of an N-Cetyl-Trimethylammonium Bromide/V<sub>2</sub>O<sub>5</sub> Nano-Composite. *Langmuir*, **17**, 1975-1982. <http://dx.doi.org/10.1021/la0009386>
- [13] Huguenin, F., Ferreira, M., Zucolotto, V., Nart, F.C., Torresi, R.M. and Oliveira, O.N. (2004) Molecular-Level Manipulation of V<sub>2</sub>O<sub>5</sub>/Polyaniline Layer-by-Layer Films to Control Electrochromogenic and Electrochemical Properties. *Chemistry of Materials*, **16**, 2293-2299. <http://dx.doi.org/10.1021/cm035171s>
- [14] Nefzi, H., Sediri, F., Hamzaoui, H. and Gharbi, N. (2012) Dielectric Properties and Electrical Conductivity of the Hybrid Organic-Inorganic Polyvanadates (H<sub>3</sub>N(CH<sub>2</sub>)<sub>4</sub>NH<sub>3</sub>)[V<sub>6</sub>O<sub>14</sub>]. *Journal of Solid State Chemistry*, **190**, 150-156. <http://dx.doi.org/10.1016/j.jssc.2012.02.013>
- [15] Jaafar, N., Naamen, S., Ben Rhaïem, H. and Ben Haj Amara, A. Functionalization and Structural Characterization of a Novel Nacrite-LiCl Hybrid Composite Material. *American Journal of Analytical Chemistry (Special Issue on X-Ray Diffraction)*. Accepted Article.
- [16] Ben Haj Amara, A. (1997) X-Ray Diffraction, Infrared and TGA/DTG Analysis of Hydrated Nacrite. *Clay Minerals*, **32**, 463-470. <http://dx.doi.org/10.1180/claymin.1997.032.3.08>
- [17] Ben Haj Amara, A., Ben Rhaïem, H. and Plançon, A. (2000) Structural Evolution of Nacrite as a Function of the Nature of the Intercalated Organic Molecules. *Journal of Applied Crystallography*, **33**, 1351-1359. <http://dx.doi.org/10.1107/S0021889800011730>
- [18] Naamen, S., Ben Rhaïem, H. and Ben Haj Amara, A. (2004) XRD Study of the Nacrite/CsCl/H<sub>2</sub>O Intercalation Complex. *Materials Science Forum*, **443-444**, 59-64. <http://dx.doi.org/10.4028/www.scientific.net/MSF.443-444.59>
- [19] Jaafar, N., Ben Rhaïem, H. and Ben Haj Amara, A. (2014) Synthesis, Characterization and Applications of a New Nano-hybrid Composite: Nacrite/MgCl<sub>2</sub>.6H<sub>2</sub>O/Ethanol. *International Conference on Composite Materials & Renewable Energy Applications (ICCMREA)*, Sousse, 22-24 January 2014, 1-6.
- [20] Jaafar, N., Ben Rhaïem, H. and Ben Haj Amara, A. (2014) Correlation between Electrochemical Impedance Spectroscopy and Structural Properties of Amorphous Tunisian Metanacrite Synthetic Material. *Advances in Materials Science and Engineering*, **2014**, Article ID: 469871. <http://dx.doi.org/10.1155/2014/469871>
- [21] Böttger, H. and Bryksin, V.V. (1985) Hopping Conduction in Solids. Akademie Verlag, Berlin, 169.
- [22] Jonscher, A.K. (1992) Universal Relaxation Law. Chapter 5, Chelsea Dielectrics Press, London.
- [23] Macdonald, J.R. (1987) Impedance Spectroscopy. John Wiley, New York.
- [24] Hummel, R.E. (1993) Electronic Properties of Materials. Springer, New York.
- [25] De Araujo, E.B., de Abreu, J.A.M., de Oliveira, R.S., de Paiva, J.A.C. and Sombra, A.S.B. (1997) Structure and Electrical Properties of Lithium Niobophosphate Glasses. *Canadian Journal of Physics*, **75**, 747-758. <http://dx.doi.org/10.1139/p97-001>
- [26] Megdiche, M., Haibado, M., Louati, B., Hlél, F. and Guidara, K. (2010) AC Electrical Properties Study and Equivalent Circuit of a Monovalent-Mixed Pyrophosphate. *Ionics*, **16**, 655-660. <http://dx.doi.org/10.1007/s11581-010-0447-9>
- [27] Réau, J.M., Rossignol, S., Tanguy, B., Rojo, J.M., Herrero, P., Rojas, R.M. and Sanz, J. (1994) Conductivity Relaxation Parameters of Some Ag<sup>+</sup> Conducting Tellurite Glasses Containing AgI or the (AgI)<sub>0.75</sub> (TlI)<sub>0.25</sub> Eutectic Mixture. *Solid State Ionics*, **74**, 65-73. [http://dx.doi.org/10.1016/0167-2738\(94\)90438-3](http://dx.doi.org/10.1016/0167-2738(94)90438-3)
- [28] Leluk, K., Orzechowski, K., Jerieb, K., Baranowskib, A., Slonkac, T. and Glowinski, J. (2010) Dielectric Permittivity of Kaolinite Heated to High Temperatures. *Journal of Physics and Chemistry of Solids*, **71**, 827-831. <http://dx.doi.org/10.1016/j.jpics.2010.02.008>
- [29] Yariv, S. (1986) Interactions of Minerals of the Kaolin Group with Cesium Chloride and Deuteration of the Complexes. *International Journal of Tropical Agricultural*, **5**, 310-322.
- [30] Michaelian, K.H., Friesen, W.I., Yariv, S. and Nasser, A. (1991) Diffuse Reflectance Infrared Spectra of Kaolinite and

- Kaolinite/Alkali Halide Mixtures. Curve-Fitting of the OH Stretching Region. *Canadian Journal of Chemistry*, **69**, 1786-1790. <http://dx.doi.org/10.1139/v91-262>
- [31] Rao, D.S. and Karat, P.P. (1994) Elastic Constants of Glasses in the System  $P_2O_5$ - $Na_2O$ - $ZnO$ . *Physics & Chemistry of Glasses*, **35**, 124.
- [32] de Oliveira, A.P.N., Leonelli, L.B.C., Manfredini, T. and Pellacani, G.C. (1996) Physical Properties of Quenched Glasses in the  $Li_2O$ - $ZrO$ - $SiO_2$  System. *Journal of the American Ceramic Society*, **79**, 1092-1097. <http://dx.doi.org/10.1111/j.1151-2916.1996.tb08552.x>
- [33] Altaf, M. and Chaudhry, M.A. (2010) Physical Properties of Lithium Containing Cadmium Phosphate Glasses. *Journal of Modern Physics*, **1**, 201-205. <http://dx.doi.org/10.4236/jmp.2010.14030>
- [34] Kim, Y.H., Yoon, M.Y., Lee, E.J. and Hwang, H.J. (2012) Effect of  $SiO_2/B_2O_3$  Ratio on Li Ion Conductivity of a  $Li_2O$ - $B_2O_3$ - $SiO_2$  Glass Electrolyte. *Journal of Ceramic Processing Research*, **13**, 37-41.
- [35] Tatsumisago, M., Hamana, A., Minami, T. and Tanaka, M. (1983) Structure and Properties of  $Li_2O$ - $RO$ - $Nb_2O_5$  Glasses (R-Ba, Ca, Mg) Prepared by Twin-Roller Quenching. *Journal of Non-Crystalline Solids*, **56**, 423-428. [http://dx.doi.org/10.1016/0022-3093\(83\)90506-9](http://dx.doi.org/10.1016/0022-3093(83)90506-9)

Scientific Research Publishing (SCIRP) is one of the largest Open Access journal publishers. It is currently publishing more than 200 open access, online, peer-reviewed journals covering a wide range of academic disciplines. SCIRP serves the worldwide academic communities and contributes to the progress and application of science with its publication.

Other selected journals from SCIRP are listed as below. Submit your manuscript to us via either [submit@scirp.org](mailto:submit@scirp.org) or [Online Submission Portal](#).

